Thermally activated growth of lath martensite in Fe–Cr–Ni–Al stainless steel

Villa, Matteo; Hansen, Mikkel Fougt; Pantleon, Karen; Somers, Marcel A. J.

Published in:
Materials Science and Technology

Link to article, DOI:
10.1179/1743284714Y.0000000583

Publication date:
2015

Document Version
Peer reviewed version

Thermally activated growth of lath martensite in Fe-Cr-Ni-Al precipitation hardenable stainless steel

M. Villa[1], M. F. Hansen[2], K. Pantleon, M. A. J. Somers[1]

1. Department of Mechanical Engineering, Technical University of Denmark, DK 2800 Kongens Lyngby, Denmark
2. Department of Micro and Nanotechnology, Technical University of Denmark, DTU Nanotech, DK 2800 Kongens Lyngby, Denmark

ABSTRACT

The austenite-to-martensite transformation in a partially hardened stainless steel containing 17wt %Cr, 7wt %Ni and 1wt % Al was investigated with Vibrating Sample Magnetometry and Electron Back-Scatter Diffraction. Magnetometry demonstrated that measurable martensite formation can be suppressed on fast cooling to 77K as well as on subsequent fast heating to 373 K. Surprisingly, martensite formation was observed during moderate heating from 77 K, instead. Electron Back-Scatter Diffraction demonstrated that the morphology of martensite is lath type. The kinetics of the transformation is interpreted in terms of a-thermal nucleation of lath martensite followed by thermally activated growth. It is anticipated that substantial autocatalytic martensite formation occurs during thermally activated growth. The observation of several retardations and accelerations of the transformation rate during slow isochronal cooling is interpreted in terms of the contribution of self-induced mechanical stabilization of austenite during martensite formation.

Keywords: *isothermal martensite; steels; sub-zero Celsius treatments; magnetometry*

INTRODUCTION

Martensite in iron-based alloys can appear as laths, characterized by an internal sub-structure with a high density of dislocations,[1,2] or as plates, which are partially[3,4] or fully[5] internally twinned[6]. Regardless of the morphology of martensite, the kinetics of martensite formation is historically described as fully nucleation-controlled,[7] with the implicit assumption of instantaneous growth of martensite upon nucleation.

However, growth of lath martensite is not instantaneous, but time-dependent and proceeds at a velocity in the range of 10^{-6} m s^{-1} to 10^{-1} m s^{-1}.[8] In Refs. 9-10 a growth rate for lath martensite formation in the order of 10^{-3} m s^{-1} was reported[9] and a martensite formation event was estimated to last 10^{-3} s.[10] Although these observations are consistent with Ref. 8 (i.e. time-dependent growth), surprisingly they were considered to corroborate nucleation-controlled descriptions.[7]

Time-dependent growth of lath martensite was followed in-situ by microscopical investigations in Ref. 11-15 and it was observed to induce time-dependent (autocatalytic) nucleation of lath martensite.[12,13,15]

After initial nucleation and growth, autocatalytic nucleation is responsible for an acceleration of the transformation.[7,16] Autocatalytic nucleation can occur either within the same austenite grain wherein martensite formation occurs or in neighbouring austenite grains.[17]

In the case of lath martensite, austenite grains are sub-divided by martensite formation at four length scales.[2,18-20] Firstly austenite grains are divided into groups of laths with the same habit plane, so-called packets. Each packet contains several blocks, which are groups of laths with the same (Kurdjumov-Sachs, K-

S) orientation relation to austenite. Block boundaries are high-angle boundaries and are either subdivided in sub-blocks of two K-S variants of martensite laths or can contain a single K-S variant. The individual laths represent the smallest level of subdivision.

In Ref. 15, continuous growth of lath martensite was observed to promote autocatalytic nucleation (mainly) within a single block of laths. In Ref. 12,13, continuous growth of lath martensite was observed to promote the generation of variants with another orientation relation with respect to austenite, leading to the formation of new blocks and packets. Finally, in-situ (synchrotron) X-ray diffraction investigations in Ref. 21 suggested that autocatalytic nucleation of lath martensite spreads the transformation over neighbouring austenite grains.

Accordingly, the applicability of fully nucleation-controlled kinetics can be questioned. In Refs. 22-24 time dependent formation of lath martensite was interpreted in terms of thermally-activated, time-dependent, nucleation, while in Refs. 25,26 time-dependent lath martensite formation was described in terms of thermally activated growth of a-thermally formed nuclei.

The purpose of the present work is to contribute to understanding the kinetics of lath martensite formation. For this purpose, a Fe-17Cr-7Ni-1Al (wt-%) stainless steel was chosen. In this steel grade the isothermal transformation of austenite into martensite[27-29] at sub-zero Celsius temperature is industrially exploited.[27,29]

Martensite formation was investigated by magnetometry, which has been demonstrated to be an accurate technique to study the martensitic transformation in iron-based alloys.[22,23,28,30-34]

Magnetometry was supplemented by Electron Back-Scatter Diffraction, which was applied to evaluate the morphology of martensite.

EXPERIMENTAL METHODS

Material and heat treatments.

The material used in the present work is a 0.15 mm thick foil 17-7 PH (precipitation hardening) stainless steel, which essentially is a Fe-17Cr-7Ni-1Al (wt-%) alloy, in rolled condition (supplied by Goodfellow Cambridge Ltd.) with the chemical composition reported in Table 1.

Austenitization of samples prepared from the rolled condition was performed in argon at 1127±10 K for 0.6 ks and was followed by cooling to 423K at an approximate average rate of 20 K min^{-1} in an argon flow. Hereafter the flow was interrupted and the samples were slowly cooled to room temperature in the sealed furnace. The as-quenched material was stored at 295±2 K for about 10 Ms (4 months) prior to magnetometry investigation; this is the controlled temperature in the room where magnetometry was performed.

Two sets of samples were prepared: a first set of three samples I, II and III; a second set of three samples A, B and C.

Table 1: Chemical composition (in wt%) of 17-7 PH steel as determined with Energy Dispersive Spectroscopy, EDS. The carbon content was measured with a LECO-CS230 Carbon analyzer

Fe	C	Si	Mn	Cr	Ni	Al
Bal.	0.09	0.5	0.7	17.3	7.3	0.8

After room temperature storage, samples I, II and III were heat treated as follows. On installing the sample in the magnetometer the samples were cooled to 290 K for 60 seconds and thereafter kept at room temperature, 295 K, for 180 s. Then, samples (one at a time) were immersed in boiling nitrogen and kept at 77 K for 60 s. From this temperature, the samples were isochronically heated to 290 K at 10 K min^{-1} (sample I), 3 K min^{-1} (sample II) and 0.15 K min^{-1} (sample III). The temperature history is shown in Fig.1a for the first 6 ks.

After room temperature storage and pre-treatment for 60 seconds at 290 K (identical to samples I, II and III) samples A, B and C were treated as follows:

A. immersion in boiling nitrogen for 60 s followed by immersion in boiling water. Thereafter, isochronal cooling from 373 K to 80 K (at 0.1 K min^{-1}) and heating to 290 K (at 10 K min^{-1}) was followed with magnetometry.

B. immersion in boiling water, followed by magnetometry investigation of isochronal cooling from 373 K to 80 K (at 0.1 K min^{-1}) and heating to 290 K (at 10 K min^{-1}).[1]

C. magnetometry investigation of isochronal cooling from 290 K to 80 K (at 0.1 K min^{-1}) and heating to 290 K (at 10 K min^{-1}).

Vibrating Sample Magnetometry, VSM.

Magnetometry was performed with a Lake Shore Cryotronics 7407 vibrating sample magnetometer equipped with a Janis SuperTran-VP continuous flow cryostat. Samples were 3 mm in diameter, 0.15 mm thick disks and were mounted onto a rigid fiber pole using non-magnetic Kapton tape. The degree of transformation was followed by recording the magnetic moment of the sample at saturation. A magnetic field of 1 Tesla was applied to bring the samples to magnetic saturation.

The absolute temperature was verified and validated at the boiling point of liquid nitrogen (i.e. 77 K) and at room temperature (i.e. 295±2 K). During thermal cycling, the temperature relative to the set point was accurate within ±0.5 K.

The molar fraction of martensite $f_{\alpha'}(t,T)$ in the material, as measured versus time, t, and temperature, T, is determined on the basis of the following assumptions:

1. the as-received (i.e. as-rolled) material is fully martensitic, as was validated by transmission X-ray diffraction;[33]
2. the *molar* fraction of martensite is proportional to the magnetic moment at magnetic saturation,[2] corrected for its dependence of temperature;[34]
3. the as-rolled sample remains stable in the temperature interval under investigation.

With these assumptions, $f_{\alpha'}(t,T)$ is given by:

$$f_{\alpha'}(t,T) = M(t,T) / M_{\alpha'}(t,T) \qquad (1)$$

where M(t,T)is the magnetic moment at saturation measured in the sample and $M_{\alpha'}(t,T)$ is the magnetic moment at saturation measured in the as-rolled material during recording of the baseline.

Electron back scatter diffraction, EBSD.

EBSD, was performed in a dual beam FEG-SEM FEI Helios Nanolab 600 SEM equipped with an EBSD system from EDAX-TSL and a Hikari camera. The measurements were performed with an electron probe

[1] The quenching steps for sample A and B were performed outside the cryostat chamber. Consequently, the content of martensite in sample A after quenching in boiling nitrogen was not measured.

[2] Note that Refs. 22, 23, 30, 31 refer to the volume fraction of martensite as determined by magnetometry. This is incorrect; magnetometry provides a measure for the molar fraction of the martensite formed.

current of 11 nA at an acceleration voltage of 18 kV, with a step size of 80nm; data were collected at four different sample locations on an overall surface area of 0.025 mm^2. The OIM TSL 6 software was used for analysis of the EBSD results.

RESULTS AND DISCUSSION

Thermally activated martensite formation.

In Fig. 1b the molar fraction of martensite, $f_{\alpha'}$, measured by magnetometry is shown as a function of temperature, T, for samples I, II, III.

The initial content of martensite in the samples just before immersion in boiling nitrogen is 15±3% (point 1 in Fig. 1b). Apparently, within experimental accuracy, fast cooling to 77 K does *not* lead to a measurable formation of martensite (point 2 in Fig. 1b - 16±3%). Martensite formation is first observed during subsequent isochronal heating. The occurrence of martensite formation during *heating* is counterintuitive and indicates convincingly that martensite formation cannot be the result of a-thermal nucleation and instantaneous growth of martensite nuclei. The observation can only be understood if martensite formation (i.e. nucleation and/or growth) is thermally activated.

The present set of experiments does *not* give an indication whether thermally activated martensite nucleation or thermally activated growth occurs. A kinetic analysis of the data in Fig.1b taking a 50% transformation as a reference (cf. Ref. 35) yielded an activation energy of 15 kJ mol^{-1}.

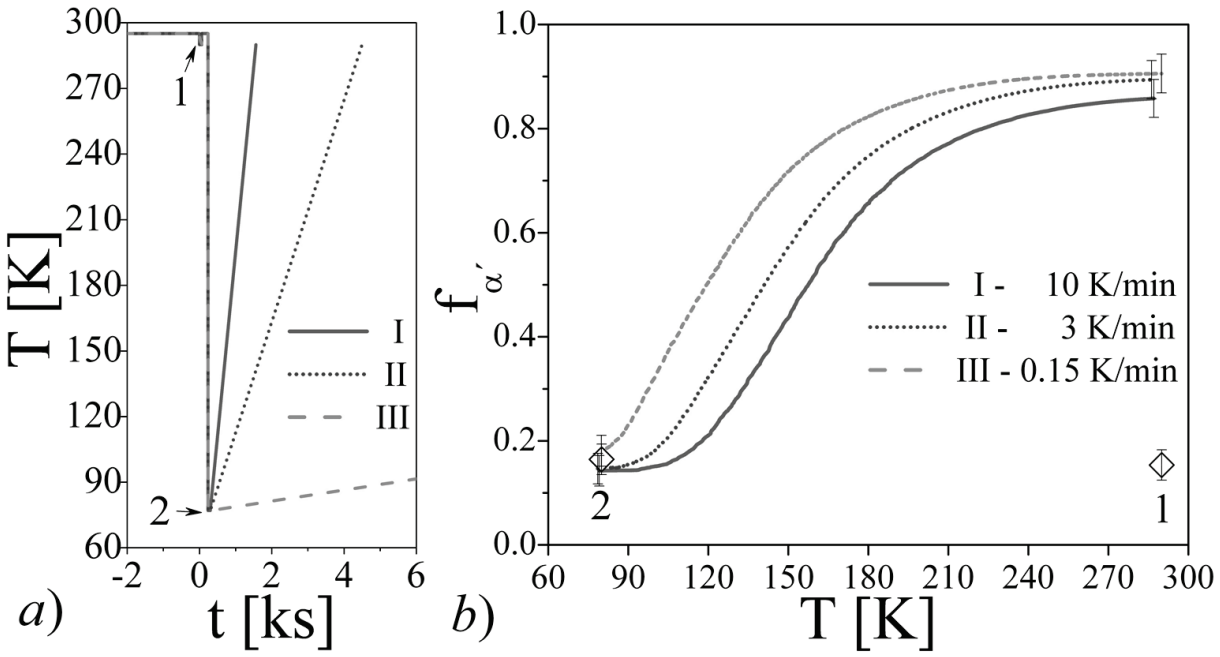

Figure 1. (a) Thermal cycles of samples I, II, and III: all samples were pre-treated at 290 K (point 1) and quenched in boiling nitrogen (point 2). The heating step terminates at 1.56 ks, 4.5 ks and 84.3 ks (out of scale) for sample I, II, and III, respectively. (b) Martensite fraction fα′ plotted versus temperature T. Black open symbols, labelled 1 and 2, refer to the average fraction of martensite determined over the different samples after pre-treatment to 290 K and after pre-treatment followed by quench in boiling nitrogen (77 K), respectively. Error bars represent reproducibility of the results according to Ref. 33.

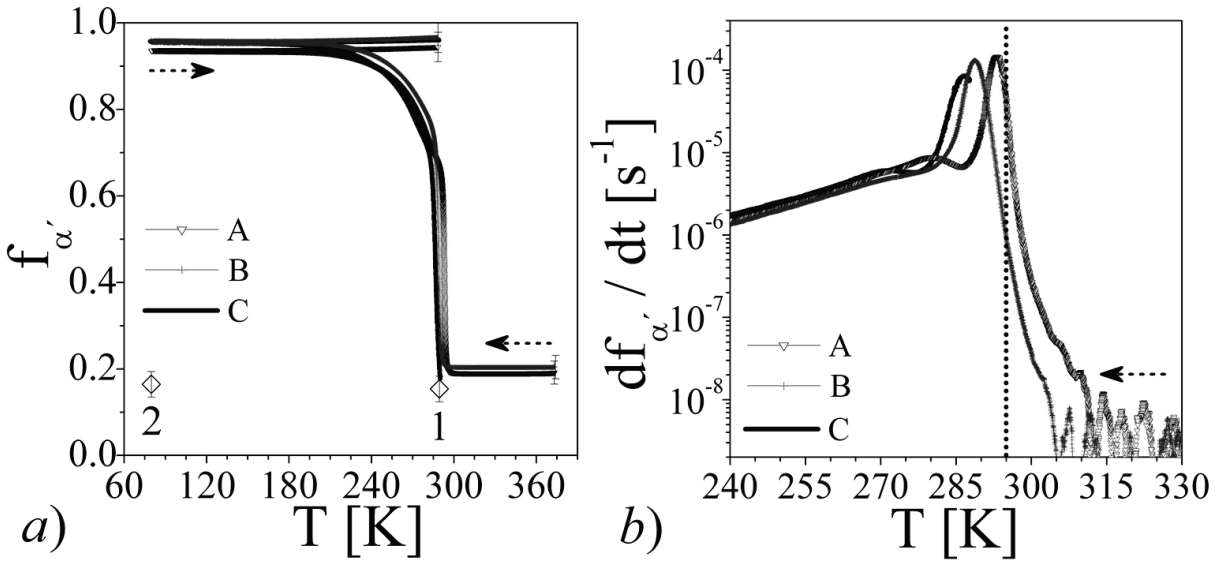

Figure 2. (a) Martensite molar fraction fα′ versus temperature T. Black open symbols, labelled 1 and 2, correspond to point 1 and 2 in Fig.1b. c) Transformation rate fα′/dt calculated within 2400 s time intervals (±2 K), versus temperature T; the vertical dotted line marks the long-term storage temperature (295±2 K).

Thermally activated growth of martensite.

The experiments presented in this section are based on the following reasoning. Provided that the transformation is *completely* suppressed on fast cooling followed by fast (re)heating above a threshold temperature were martensite formation is inhibited by thermodynamics, martensite formation during a second, slower, cooling step is:

1. *not* influenced by the initial thermal step, in the case that the kinetics of the transformation is controlled by time-dependent nucleation;
2. strongly influenced by the initial thermal step if the kinetics of the transformation is controlled by time-dependent growth of nuclei that have developed a-thermally during the initial cooling sequence.

Samples A, B and C were heat treated accordingly.

The fractions of martensite measured during the different controlled thermal cycles are collected in Fig. 2a. The transformation rate on controlled cooling in the temperature interval 330 K to 240 K is shown in Fig. 2b.

Martensite formation appears suppressed on fast (re)heating to 373 K, both from 290 K and from 77 K.

The slightly higher fraction of martensite at 373 K, (i.e. 19±3%) as compared to point 1 and 2 (i.e. 15±3%) is still within experimental error.

On isochronal cooling, neither sample A nor sample B showed a measurable transformation down to 310 K (Fig. 2b). The criterion for a measurable transformation is taken as $df_{\alpha'}/dt > 2 \cdot 10^{-8}\ s^{-1}$, which is a value safely larger than the noise level (see arrow in Fig 2b).

At 310 K, martensite formation is observed to start slowly in sample A, while martensite formation in sample B is first observed at 304 K. The onset of the transformation in samples A and B at temperatures well-above the long-term storage temperature of 295±2 K after austenitization, cannot be reconciled with a-thermal nucleation; neither can it be a consequence of thermally activated nucleation of martensite. These results

indicate that both the pre-treatment from 295 K to 290 K (sample B) and the additional cooling to 77 K (sample A) have led to the development of martensite nuclei, and that these nuclei are thermally activated to grow in the isochronal cooling stage at a temperature higher than the storage temperature. The instantaneous martensite formation as observed in sample C on cooling from 290 K corroborates that cooling from 295 K to 290 K has indeed led to the development of martensite nuclei.

The observation that measurable martensite formation starts at a higher temperature in sample A than in sample B (Fig. 2), is explained by a faster transformation in sample A, resulting from a larger number of nuclei formed upon cooling to 77 K (sample A) as compared to cooling to 290 K (sample B). During continuous cooling, the transformation rate reaches a maximum at 293 K, 289 K and 287 K for samples A, Band C, respectively. After this maximum, the transformation rate in samples A and C shows a deceleration followed by an acceleration, while for sample B the transformation decelerates monotonically. The occurrence of a deceleration of the transformation followed by a second acceleration is *abnormal* after Refs. 36-39. It is anticipated that abnormal transformation indicates the presence of autocatalytic nucleation.

The results of orientation image microscopy of samples A and B are shown in Figs. 3. A quantitative evaluation of the EBSD results (Fig.4) was obtained for the areas separated by high angle grain boundaries, i.e. a misorientation larger than 15°, which represent blocks in the lath martensite microstructure.

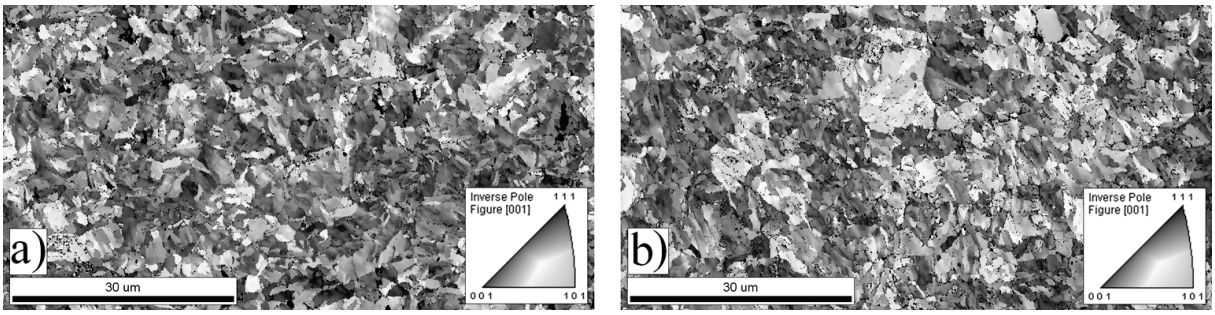

Figure 3. EBSD investigation: orientation image microscopy: a) sample A; b) sample B. The reported orientation images represent 15% of the area investigated by EBSD.

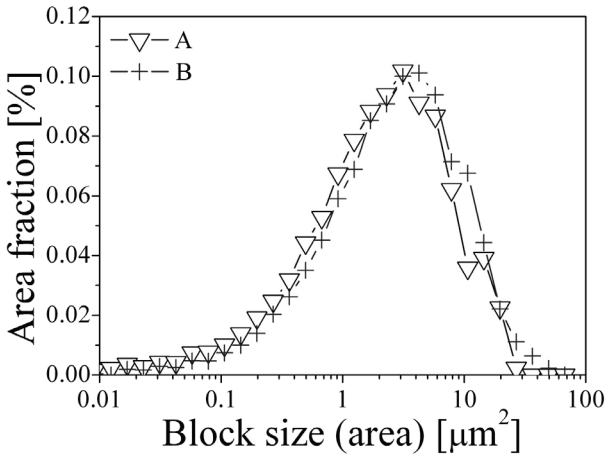

Figure 4. Block size distribution (area) for the samples A and B, respectively. Data refers to an overall surface area of 0.025 mm-2 per sample.

Evidently, the quantitative size distribution of martensite regions in samples A and B is identical within experimental accuracy (Fig. 4). This indicates that the higher number of nuclei in sample A as compared to sample B is not reflected in the microstructure after completed transformation. Hence, it has to be concluded that additional nucleation has occurred in sample B during isochronal cooling.

In principle, such nucleation could have taken place purely a-thermally. However, since the largest part of the transformation is accomplished within a very narrow temperature range for all investigated samples (cf. Fig. 2b), it is anticipated that autocatalytic nucleation has contributed substantially to the transformation.

Abnormal martensite formation.

In this section, abnormal martensite formation is discussed in relation to the abnormal *massive* transformation of austenite into ferrite, as described in Refs. 36-39. The latter is introduced first.

At the beginning of the massive transformation, nucleation of ferrite at several locations in the sample is followed by thermally activated growth. The strain energy which is introduced *locally* in the system as a consequence of the volume misfit between ferrite and austenite (i.e. the introduction of shear stresses), promotes autocatalytic nucleation of ferrite in front of the ferrite -austenite interface.[36] Autocatalytic nucleation yields a strong acceleration of the transformation, which comes to a halt when the strain energy introduced in the system by the transformation itself, *averaged* over the entire sample (i.e. the sum of interfacial energies, introduction of crystal defects and build up of hydrostatic pressure in austenite), equals the chemical driving force. Thereafter, an increment of the driving force upon continuous cooling is necessary to initiate a new (autocatalytic) nucleation event.

In the present case, at 310 K, several (infinitively small) nuclei of lath martensite are present in the material as a consequence of a-thermal nucleation in the first cooling step. The number of nuclei differs for samples A and B and is largest in sample A, because of the significantly lower temperature reached in sample A during cooling (i.e. 77 K versus 290 K).

On cooling below 310 K, martensite starts to grow. Evidently, the driving force at 310 K is sufficient to compensate for the interfacial energy and the elastic and plastic strain energy terms associated with martensite formation and the frictional work accompanying the movement of the austenite/martensite interface.[40,41] For a relatively small transformed fraction, martensite formation introduces shear[21] and tensile dilatational[42] stresses in the surrounding austenite matrix, which exceeds the other energy terms in austenite accompanying martensite formation and *promotes* the driving force for (autocatalytic) martensite formation.

For a relatively large transformed fraction, (retained) austenite regions become encaged by martensite. Then additional martensite formation induces compressive strain energy terms in austenite,[42-44] which *counteracts* the driving force for martensite formation[45-47] (i.e. mechanical stabilization of austenite[8] occurs during martensite formation).

The compressive strain energy in austenite suppresses martensite nucleation and results in a deceleration of the transformation. However, martensite formation does not completely stop, because growth of pre-existing nuclei can still occur.

A new acceleration of the martensite formation occurs when additional undercooling leads to a further increase of the driving force. At this point, provided that there is enough austenite to transform, an increase in the nucleation rate may yield a new acceleration of the transformation, as is observed at 280 K in sample A (and C). The reason that this acceleration is not observed for sample B, could be the lower fraction of untransformed austenite as compared to sample A (and C) at this point.

To summarize, autocatalytic nucleation of martensite is promoted by continuous growth of the martensite areas. The combined effect of autocatalytic nucleation and self-induced mechanical stabilization of austenite yield abnormal transformation, characterized by repeated acceleration and deceleration of the transformation.

CONCLUSIONS

Martensite development in a 17-7 PH (i.e. 17wt %Cr, 7wt %Ni and 1wt % Al) stainless steel was investigated with magnetometry and Electron Back-Scatter Diffraction. It was observed that fast cooling to 77 K, well below M_s, and fast heating from below M_s to a temperature well above M_s did not lead to a measurable formation of martensite. Instead martensite develops during controlled cooling from above M_s or controlled heating from a temperature well below M_s (77 K).

The results can be interpreted consistently assuming that a-thermal (mainly autocatalytic) nucleation occurs, followed by thermally activated growth of the martensite nuclei. The activation energy for thermally activated martensite growth was assessed at 15 $kJ.mol^{-1}$.

The observation of abnormal lath martensite formation is reported on continuous cooling. Abnormal transformation is interpreted in terms of self-induced mechanical stabilization of austenite during martensite formation.

REFERENCES

1. K. Wakasa, C.M. Wayman, *"Crystallography and Morphology of Ferrous Lath Martensite"*, Acta Metal., 1981, 29, 991-1001.
2. S. Morito, X. Huang, T. Furuhara, T. Maki, N. Hansen, *"The Morphology and Crystallography of Lath Martensite in Steel"*, Acta Mater., 2006, 54, 5323-5331.
3. K. Shimizu, M. Oka, C.M. Wayman, *"The association of martensite platelets with austenite stacking faults in an Fe-8Cr-1C alloy"*, Acta Metall., 1970, 18:9, 1005-1011.
4. A. Shibata, S. Morito, T. Furuhara, T. Maki, *"Substructures of lenticular martensites with different martensite start temperatures in ferrous alloys"*, Acta Mater., 2009, 57:2, 483-492.
5. T. Maki, C.M. Wayman, *"Substructure of ausformed martensite in Fe-Ni and Fe-Ni-C alloys"*, Metall. Trans., 1976, 7A:9, 1511-1518.
6. G. Krauss, A.R. Marder, *"The morphology of martensite in iron alloys"*, Metall. Trans., 1971, 9:2, 2343-2357.
7. N.N. Thadhani, M.A. Meyers, *"Kinetics of isothermal martensitic transformation"*, Progress in Mater. Sci., 1986, 30:1, 1-37.
8. Z. Nishiyama, "*Martensitic Transformation*", 1978, New York: Academic Press.
9. K. Takashima, Y. Higoa, S. Nunomura, *"The propagation velocity of the martensitic transformation in 304 stainless steel"*, Philosophical Mag., 1984, 49A:2, 231-241.
10. F. Foerster, E. Scheil, "*Acoustical study of formation of martensite needles"*, Naturwissenschaften, 1936, 28:9, 245-247.
11. J.H. Lee, T. Fukuda, T. Kakeshita, *"Isothermal Martensitic Transformation in Sensitized SUS304 Austenitic Stainless Steel at Cryogenic Temperature"*, Mater. Trans., 2009, 50:3 473-478.
12. D-Z. Yang, C.M. Wayman, *"Slow growth of isothermal lath martensite in an Fe&z.sbnd;21N&z.sbnd;4Mn alloy"*, Acta Metall., 1984, 32:6, 949-954.
13. T. Kakeshita, K. Kuroiwa, K. Shimizu,T. Ikeda, A. Yamagishi, M. Date, *"Effect of magnetic fields on athermal and isothermal martensitic transformations in Fe-Ni-Mn alloys"*, Mater. Trans. JIM., 1993, 34:5, 415-422.
14. T. Araki, K. Shibata, K. Asakura, H. Wada, *"Direct observation of the gamma yields alpha prime isothermal martensitic transformation of iron alloys in electron microscope"*, ISIJ., 1975, 15:4, 175-184.

15. J.M. Marder, A.R. Marder, *"Formation of low Carbon Martensite in Fe-C Alloys"*, ASM Transaction, 1969, 62:1, 1-10.
16. S.R. Pati, M. Cohen, *"Kinetics of isothermal martensitic transformations in an iron-nickel-manganese alloy"*, Acta Meta., 1971, 19:12, 1327-1332.
17. P.R. Rios, J.R.C. Guimarães, *"Formal Analysis of Isothermal Martensite Spread"*, Mater. Research, 2008, 11:1, 103-108.
18. H. Kitahara, R. Ueji, N. Tsuji, Y. Minamino, *"Crystallographic features of lath martensite in low-carbon steel"*, Acta Mater., 2006, 54:5, 1279–1288.
19. S. Morito, H. Tanaka, R. Konishi, T. Furuhara, T. Maki, *"The morphology and crystallography of lath martensite in Fe-C alloys"*, Acta Mater., 2003, 51:6, 1789–1799.
20. T. Furuhara, N. Takayama, G. Miyamoto, *"Key Factors in Grain Refinement of Martensite and Bainite"*, Mater. Sci. Forum, 2010, 638-642, 3044-3049.
21. D. San Martin, E. Jimenez-Melero, J.A. Duffy, V. Honkimaki, S. van der Zwaag, N.H. van Dijk, J. *"Real-time synchrotron X-ray diffraction study on the isothermal martensite transformation of maraging steel in high magnetic fields"*, Appl. Cryst., 2012, 45, 718-757.
22. D. San Martin, K.W.P Aarts, P.E.J. Rivera-Diaz-del-Castillo, N.H. van Dijk, E. Bruck, S. van der Zwaag, *"Isothermal martensitic transformation in a 12Cr-9Ni-4Mo-2Cu stainless steel in applied magnetic fields"*, J. Magnetism and Magn. Mater., 2008, 320:10, 1720-1728.
23. D. San Martin, N.H. van Dijk, E. Jimenez-Melero, E. Kampert, U. Zeitler, S. van der Zwaag, *"Real-time martensitic transformation kinetics in maraging steel under high magnetic fields"*, Mat. Sci. Eng., 2010, 527A:20, 5241-5245.
24. J.R.C. Guimaraes, P.R. Rios, *"Unified model for plate and lath martensite with athermal kinetics"*, Metall. and Mater. Trans., 2010, 41A:8:, 1928-1935.
25. Y. Liu, L. Zhang, F. Sommer, E.J. Mittemeijer, *"Kinetics of martensite formation in substitutional Fe-Al alloys: Dilatometric analysis"*, Metall. and Mater. Trans., 2013, 44A:3, 1430-1440.
26. D. Kim, J.G. Speer, B.C. De Cooman, *"Isothermal Transformation of a CMnSi Steel Below the M-S Temperature"*, Metall. and Mater. Trans., 2011, 42A:6, 1575-1585.
27. D.C. Ludwigson, A.M. Hall, "*The Physical Metallurgy of Precipitation-Hardenable Stainless Steel"*, 1959, Defence Metals information center, Report III.
28. T.D. Kubyshkina, L.M. Pevzner, Ya. M. Potak, *"The martensitic transformation in stainless steels of the austenitic-martensitic class"*, Metallov. i Term. Obrabotka, 1960, 8:2, 9-17.
29. C.J. Slunder, A.F. Hoenie, A.M. Hall, "*Thermal and Mechanical Treatment for Precipitation-Hardening Stainless Steel"*, 1967, NASA, Washington, D.C..
30. L. Zhao, N.H. van Dijk, E. Bruck, J. Sietsma, S. van der Zwaag, *"Magnetic and X-ray diffraction measurements for the determination of retained austenite in TRIP steels"*, Mater. Sci. Eng., 2001, 313A:1-2, 145-152.
31. M. Radu, J. Valy, A.F. Gourgues, F. Strat, A. Pineau, *"Continuous magnetic method for quantitative monitoring of martensitic transformation in steels containing metastable austenite"*, Scripta Mater., 2005, 52:6, 525-530.
32. T. Koyano, *"Isothermal martensitic transformation of γ-FeN in a magnetic field"*, Mater. Trans., 2003, 44:12, 2541-2544.
33. M. Villa, *"Isothermal martensite formation"*, PhD Thesis, Lyngby, Denmark: The Technical University of Denmark, 2013, submitted.
34. A. Stojko, *"The effect of cryogenic treatment on structural and phase transformations in iron-carbon martensite"*, PhD Thesis; Lyngby, Denmark: The Technical University of Denmark, 2006.
35. E.J. Mittemeijer, *"Analysis of the kinetics of phase transformations"*, J. of Mater. Sci, 1992, 27:15, 3977-3987.
36. Y.C. Liu, F. Sommer, E.J. Mittemeijer, *"Abnormal austenite-ferrite transformation behaviour in substitutional Fe-based alloys"*, Acta Mater., 2003, 51:2, 507-519.
37. Y.C. Liu, F. Sommer, E.J. Mittemeijer, *"Kinetics of the abnormal austenite-ferrite transformation behaviour in substitutional Fe-based alloys"*, Acta Mater., 2004, 52:9, 2549-2560.
38. Y.C. Liu, F. Sommer, E.J. Mittemeijer, *"Abnormal austenite-ferrite transformation kinetics of ultra-low-nitrogen Fe-N alloy"*, Metall. And Mater. Trans., 2008, 39A:10, 2306-2318.

39. Y.C. Liu, F. Sommer, E.J. Mittemeijer, *"Abnormal austenite-ferrite transformation behavior in pure iron"*, Chinese Sci. Bullettin, 2004, 49:9, 972-975.
40. M. Grujicic, G.B. Olson, W.S. Owen, *"Mobility of martensitic interfaces"*, Metall. Trans., 1985, 16A:10, 1713-1722
41. D. Eshelby, *"The determination of the elastic field of an ellipsoidal inclusion, and related problems"*, Proc. Roy. Soc. (London) A 241 (1957) 376–396
42. V.M. Yershov, N.L. Oslon, *"Change in linear expansion coefficient of austenite on transformation to martensite"*, Fiz. Met. Metalloved, 1968, 25:5, 874-881
43. M. Villa, K. Pantleon, M.A.J. Somers, *"Martensitic transformation and stress partitioning in a high-carbon steel"*, Scr. Mater., 2012, 67:6, 621-624.
44. K. Ja. Golovchiner, *"Changes in the lattice parameter of austenite during martensitic transformation of steel"*, Phys. Metals Metallogr., 1974, 37:2, 126
45. J.R. Pati, M. Cohen, *"Criterion for the action of applied stress in the martensitic transformation"*, Acta Mater., 1953, 1:5, 531-538
46. T. Kakeshita, K. Kuroiwa, K. Shimizu, T. Ikeda, A. Yamagishi, M.A. Date, *"A New Model Explainable for Both the Athermal and Isothermal Natures of Martensitic Transformations in Fe-Ni-Mn Alloys"*, Mater. Trans. JIM., 1993, 34:5, 423-428.
47. T. Kakeshita, T. Saburi, K. Shimizu, *"Effects of hydrostatic pressure and magnetic field on martensitic transformations"*, Mater. Sci. Eng., 1999, A273-275, 21-39.